analytical chemistry

pubs.acs.org/ac Article

Coenzyme-Mediated Electro-RAFT Polymerization for Amplified Electrochemical Interrogation of Trypsin Activity

Qiong Hu, Luofeng Su, Zhuohua Chen, Yanyu Huang, Dongdong Qin, and Li Niu*

Cite This: *Anal. Chem.* 2021, 93, 9602−9608 Read Online

ACCESS | Metrics & More | Article Recommendations | Supporting Information

ABSTRACT: Trypsin is a key proteolytic enzyme in the digestive system and its abnormal levels are indicative of some pancreatic diseases. Taking advantage of the coenzyme-mediated electrografting of ferrocenyl polymers as a novel strategy for signal amplification, herein, a signal-on cleavage-based electrochemical biosensor is reported for the highly selective interrogation of trypsin activity at ultralow levels. The construction of the trypsin biosensor involves (i) the immobilization of peptide substrates (without free carboxyl groups) via the N-terminus, (ii) the tryptic cleavage of peptide substrates, (iii) the site-specific labeling of the reversible addition−fragmentation chain transfer (RAFT) agents, and (iv) the grafting of ferrocenyl polymers through the electro-RAFT (eRAFT) polymerization, which is mediated by potentiostatic reduction of nicotinamide adenine dinucleotide (NAD^+) coenzymes. Through the NAD^+-mediated eRAFT (NAD^+-eRAFT) polymerization of ferrocenylmethyl methacrylate (FcMMA), the presence of a few tryptic cleavage events can eventually result in the recruitment of a considerable amount of ferrocene redox tags. Obviously, the NAD^+-eRAFT polymerization is low-cost and easy to operate as a highly efficient strategy for signal amplification. As expected, the as-constructed biosensor is highly selective and sensitive toward the signal-on interrogation of trypsin activity. Under optimal conditions, the detection limit can be as low as 18.2 μU/mL (~72.8 pg/mL). The results also demonstrate that the as-constructed electrochemical trypsin biosensor is applicable to inhibitor screening and the interrogation of enzyme activity in the presence of complex sample matrices. Moreover, it is low-cost, less susceptible to false-positive results, and relatively easy to fabricate, thus holding great potential in diagnostic and therapeutic applications.

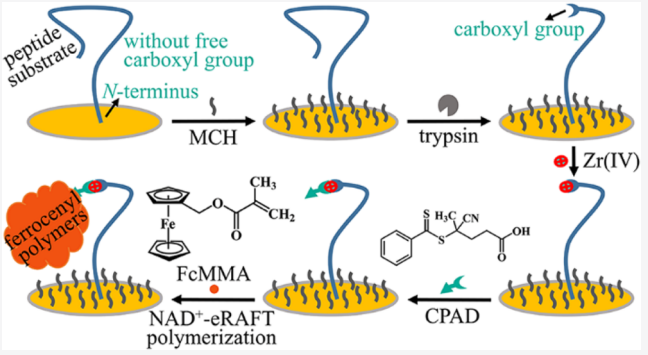

Trypsin is the most important proteolytic enzyme in the digestive system for breaking down proteins into smaller fragments. As an endopeptidase, it prefers to catalyze the hydrolysis of peptide bonds in proteins and peptides at the carboxyl side of lysine (Lys) or arginine (Arg) residue.[1] Trypsin is secreted as the inactive precursor trypsinogen in the exocrine cells of the pancreas, and it is well known that the abnormal levels of trypsin in biological fluids are closely associated with various pancreatic diseases, such as acute pancreatitis, cystic fibrosis, and pancreatic cancer. For example, trypsin is absent from the urine of healthy individuals, whereas the mean trypsin concentration in the urine of pancreas transplant patients is 84.4 μg/mL;[2] in healthy individuals, the concentration of serum trypsin ranges from 138 to 406 ng/mL, while in the patients suffering from acute pancreatitis, it can be up to 6.5 μg/mL.[3] Therefore, low-cost and easy-to-operate methods for the selective and sensitive interrogation of trypsin activity and inhibitor screening are highly desired for diagnostic and therapeutic applications.

For the interrogation of trypsin activity, various cleavage-based methods have been established,[4−6] such as gel electrophoresis,[7] fluorescence,[8] colorimetry,[9] photoelectrochemistry (PEC),[10] quartz crystal microbalance (QCM),[11] electrochemiluminescence (ECL),[12] mass spectrometry (MS),[13] surface-enhanced Raman scattering (SERS),[14] nanopores,[15] and electrochemical biosensors.[16−20] These methods typically involved the tryptic cleavage of synthetic substrates, which consist of a short peptide fragment of known sequence specific for trypsin. In recent years, much effort has been devoted to developing cleavage-based electrochemical biosensors, by virtue of their advantages of being low-cost, portable, highly selective and sensitive, and compatible with microfabrication techniques. The simplest cleavage-based electrochemical trypsin biosensors were presented by Cao et al.,[16] Adjémian et al.,[17] and González-Fernández et al.[18] using the cationic peptides, ferrocene (Fc)-labeled peptides, and

Received: April 26, 2021
Accepted: June 14, 2021
Published: June 29, 2021

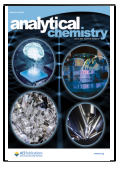

https://doi.org/10.1021/acs.analchem.1c01766
Anal. Chem. 2021, 93, 9602−9608

methylene blue (MB)-labeled peptides, respectively, as the immobilized substrates for trypsin. In the first method, the tryptic removal of the terminal cationic residues could largely alleviate the blocking effect of the peptide layer against the positively charged $[Ru(NH_3)_5Cl]^{2+}$ redox probes, rendering the signal-on interrogation of trypsin activity. In the latter two methods, the cleavage of trypsin substrates resulted in the release of redox tags; that is, they are signal-off methods and thus are susceptible to false-positive results.[20,21] These three methods mentioned above are low-cost and relatively easy to operate; however, their limits of detection (LODs) are not satisfactory. For better detection sensitivity, functional gold nanoparticles (AuNPs) have been explored by Liang et al. as carriers to load numerous redox tags.[19] In this method, the peptide substrate was preconjugated with an oligonucleotide fragment through the biotin−streptavidin interaction, and then the oligonucleotide−AuNPs−thionine conjugate was labeled via DNA hybridization. Hence, each cleavage event could bring about the loss of numerous thionine redox tags, allowing for the signal-off interrogation of trypsin activity at ultralow levels. In addition to the disadvantage of being susceptible to false-positive results, the high cost and complexity are adverse to its broad applications. Consequently, there is a need for low-cost and easy-to-operate strategy for the amplified electrochemical interrogation of trypsin activity at ultralow levels.

As we know, the chain of a polymer can be composed of thousands to millions of repeated units.[22] Of great interest is that the side chains of a polymer can serve as the functional sites to load numerous redox tags for signal amplification.[23−26] Through the in situ grafting of polymers using Fc-containing monomers, for example, a large number of Fc tags can be recruited.[27] Inspired by this consideration, in this work, we report the use of the coenzyme-mediated electrografting of ferrocenyl polymers through the electro-RAFT (eRAFT) polymerization as a novel strategy for signal amplification for the signal-on electrochemical interrogation of trypsin activity at ultralow levels. As one of the most studied and versatile reversible deactivation radical polymerization methods for the controlled preparation of polymer products with well-defined architecture and low dispersity, reversible addition−fragmentation chain transfer (RAFT) polymerization is typically mediated by RAFT agents[28] in the form of a thiocarbonylthio compound.[29] RAFT polymerization is well compatible with a wide range of solvents and vinyl monomers[26] and can be initiated and sustained by the thermal decomposition of a radical initiator.[30−32] However, thermal initiation requires elevated reaction temperatures (50−70 °C),[26] while limiting the degree of control and generating initiator-derived byproducts.[28,33] To avoid these defects, alternative methods to initiate and sustain RAFT polymerization in the absence of exogenous radical sources and under mild conditions are more attractive, especially through the activation of RAFT agents by redox mediators into radical species.[34−36] This is because it would be compatible with biological or thermoresponsive systems and the polymerization of some functional monomers while allowing for spatiotemporal control over the polymerization process.[37] In this work, the initiation and maintenance of the RAFT polymerization is mediated by electroreduction of the nicotinamide adenine dinucleotide (NAD^+) coenzyme,[38,39] which is a ubiquitous electron-transfer mediator in metabolism. Specifically, the electroreduction of the NAD^+ coenzyme at room temperature mediates the activation of RAFT agents into radical species, which then react with vinyl monomers to form polymeric chains,[38] without the need for an exogenous radical source. For the interrogation of trypsin activity, the peptide substrates without free carboxyl groups are end-tethered via the N-terminus. The free carboxyl termini generated from the tryptic cleavage events are used for the labeling of RAFT agents via carboxylate−Zr(IV)−carboxylate chemistry. Through the NAD^+-mediated eRAFT (NAD^+-eRAFT) polymerization of ferrocenylmethyl methacrylate (FcMMA) monomers, a large number of ferrocenyl polymers can be grafted from the cleaved sites. Hence, the presence of an ultralow level of trypsin activity could eventually result in the recruitment of a considerable amount of Fc redox tags. Obviously, the NAD^+-eRAFT polymerization is low-cost and easy to operate as a highly efficient strategy for signal amplification. The results also demonstrate that the as-constructed cleavage-based electrochemical trypsin biosensor is highly selective and sensitive and applicable to inhibitor screening and the interrogation of tryptic activity in the presence of complex sample matrices. In addition, it is low-cost, less susceptible to false-positive results, and relatively easy to fabricate, thus holding great potential in diagnostic and therapeutic applications.

EXPERIMENTAL SECTION

Materials and Reagents. A peptide substrate, $CGGSSRGG\text{-}CONH_2$, was offered by Shanghai Science Peptide Biological Technology Co., Ltd. (Shanghai, China). Trypsin (from porcine pancreas; specific activity, 250 units (U)/mg; molecular weight, 23.8 kDa) and chymotrypsin were obtained from Sangon Biotech (Shanghai) Co., Ltd. (Shanghai, China). Thrombin (from bovine plasma), ferrocenylmethyl methacrylate (FcMMA), and α-fetoprotein (AFP, from human fetal cord serum) were purchased from Beijing Solarbio Science & Technology Co., Ltd. (Beijing, China), Shanghai Pharmlead Inc. (Shanghai, China), and Shanghai Linc-Bio Science Co., Ltd. (Shanghai, China), respectively. Pepsin (from porcine gastric mucosa), hemoglobin human, β-nicotinamide adenine dinucleotide hydrate (NAD^+), zirconium dichloride oxide octahydrate ($ZrOCl_2$), albumin (from human serum), Bowman−Birk inhibitor (BBI, from soybean), and 6-mercapto-1-hexanol (MCH) were offered by Sigma-Aldrich. Lithium perchlorate trihydrate ($LiClO_4$) and 4-cyano-4-(phenylcarbonothioylthio)pentanoic acid (CPAD) were provided by Shanghai Aladdin Bio-Chem Technology Co., Ltd. (Shanghai, China). Potassium hexafluorophosphate (KPF_6) and tris(hydroxymethyl)aminomethane (Tris) were bought from J&K Scientific Ltd. (Shanghai, China). *N*,*N*-Dimethylformamide (DMF) and other chemicals, analytical grade or higher, were used as received. Milli-Q water (≥18.25 MΩ cm) was used as the water source.

The electrografting solution was a mixture of FcMMA (0.5 mM) and NAD^+ (0.5−1.25 μM) in 25% DMF. The solution for electrochemical impedance spectroscopy (EIS) was 5.0 mM $[Fe(CN)_6]^{3-/4-}$ in 0.1 M KNO_3.

Apparatus. The morphology of the as-modified gold electrode was studied using a JSM-7100F field emission scanning electron microscope (JEOL), with an accelerating voltage of 15 kV. Electrochemical experiments were performed with a routine three-electrode system at room temperature. The working electrode (WE) is a modified gold electrode (3.0 mm), the reference electrode (RE) is a saturated calomel electrode (SCE), and the counter electrode (CE) is a platinum wire. Voltammetric experiments were performed on a

https://doi.org/10.1021/acs.analchem.1c01766
Anal. Chem. 2021, 93, 9602−9608

CHI760E electrochemical workstation (CH Instruments). EIS experiments were carried out on a Reference 600+ potentiostat/galvanostat (Gamry Instruments) at the open-circuit potential by applying an *ac* voltage of 10 mV amplitude in a frequency range from 100 kHz to 0.1 Hz.

Electrochemical Interrogation of Trypsin Activity. First, the gold electrode was polished with 0.3 μm alumina slurry and sonicated sequentially in ethanol and Milli-Q water. Then, it was soaked in a fresh piranha solution (a 3:1 v/v mixture of 98% H_2SO_4 and 30% H_2O_2; caution: it is highly corrosive and must be handled with great care) at 75 °C for 30 min, followed by a thorough rinse with Milli-Q water. After an electrochemical cleaning in 0.5 M H_2SO_4 by potential cycling between −0.3 and 1.5 V (final potential, 0.6 V), it was cleaned in 0.5 M NaOH at −1.2 V for 30 s and sonicated in Milli-Q water. After drying with nitrogen, it was incubated with 10 μL of the peptide substrate at 37 °C for 45 min. The obtained electrode (abbreviated as Au/P) was backfilled with 2.0 mM MCH (50% ethanol) at 37 °C for 15 min. After the sequential rinse with ethanol and Milli-Q water, Au/MCH/P was incubated with 10 μL of trypsin (50 mM Tris−HCl, 1.0 mM $CaCl_2$, pH 7.6) at 37 °C for 1.0 h. After a rinse with Milli-Q water, Au/MCH/P_{COOH} was soaked in 5.0 mM $ZrOCl_2$ (20% ethanol) at 37 °C for 15 min and rinsed with Milli-Q water. Au/MCH/P_{COOH}/Zr(IV) was incubated with 1.0 mM CPAD (30% ethanol) at 37 °C for 15 min and rinsed with ethanol and Milli-Q water. Further, Au/MCH/P_{COOH}/Zr(IV)/CPAD was soaked in the electrografting solution, followed by electrografting under moderate stirring for 1.5 h. After a thorough rinse with ethanol and Milli-Q water, Au/MCH/P_{COOH}/Zr(IV)/CPAD/Fc was interrogated in 0.5 M $LiClO_4$ (for its ability to stabilize the Fc^+ cation[27]) by square wave voltammetry (SWV) with a potential increase of 4.0 mV and a potential amplitude of 25 mV.

RESULTS AND DISCUSSION

Principle of the Electrochemical Interrogation of Trypsin Activity. The principle is illustrated in Scheme 1.

Scheme 1. Principle of the Cleavage-Based Electrochemical Interrogation of Trypsin Activity through NAD$^+$-eRAFT Polymerization

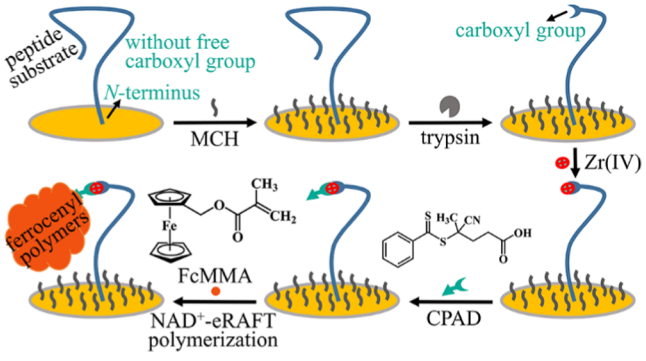

The peptide substrates are first tethered onto the electrode surface via the N-terminal cysteine (Cys) residue; they are free of carboxyl groups. The free carboxyl termini generated from the tryptic cleavage events can be used for the site-specific labeling of CPAD RAFT agents via well-established carboxylate−Zr(IV)−carboxylate chemistry.[21] Further, electroreduction of the NAD$^+$ coenzymes mediates the fragmentation of the CPAD RAFT agents (with a general structure of S═C(Z)S−R, in which R is a radical leaving group and Z is an activating group) into an anionic fragment (S═C(Z)S$^-$) and a radical species ($R^\bullet$).[28,38] It is noteworthy that the CPAD RAFT agents in this work are tethered to the C-terminus of the cleaved peptides via the carboxyl group in the R group. Hence, the $R^\bullet$ radicals would be tethered to the electrode surface. Subsequently, the propagation of the $R^\bullet$ radicals by repeatedly reacting with FcMMA monomers would result in the de novo electrografting of ferrocenyl polymers. Thus, the presence of a few cleaved sites can recruit a considerable amount of Fc redox tags, allowing for the signal-on electrochemical interrogation of trypsin activity at ultralow levels. Obviously, the NAD$^+$-eRAFT polymerization is low-cost and easy to operate as a strategy for signal amplification. Taking together, the integration of the electrografting of ferrocenyl polymers through NAD$^+$-eRAFT polymerization into the cleavage-based electrochemical biosensor is highly applicable to the highly selective interrogation of trypsin activity at ultralow levels.

Redox Properties of NAD$^+$ and CPAD. The NAD$^+$-eRAFT polymerization was performed in the presence of the NAD$^+$ coenzyme as the redox mediator. Previous reports have shown that the cathodic electrolysis can also irreversibly cleave RAFT agents at the weak C−S bond to generate two anionic fragments,[35] leading to various side reactions without generating any long-lived free radicals.[28,36] To avoid this, the reduction wave of the redox mediator should not overlap with that of the RAFT agent.[34] For the efficient outer-sphere electron transfer from the reduced mediators to RAFT agents, the reduction potential of the redox mediator should be higher than that of the RAFT agent by less than 0.5 V.[28] To show the suitability of the NAD$^+$ coenzyme as a redox mediator for eRAFT polymerization, cyclic voltammetry (CV) was applied to investigate the reduction potentials of the NAD$^+$ coenzyme and the CPAD RAFT agent. The CV of the NAD$^+$ coenzyme presented a reduction peak at −0.75 V (Figure 1),

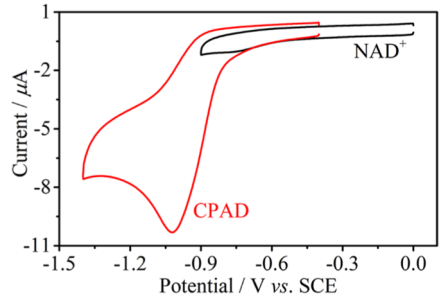

Figure 1. CVs of the NAD$^+$ coenzyme and the CPAD RAFT agent. The concentration of NAD$^+$ and CPAD was 1.0 mM. The supporting electrolyte was a mixture of 0.1 M KPF_6 and DMF (v/v = 1/1, nitrogen saturated).

corresponding to the one-electron reduction of the NAD$^+$ coenzyme into a radical species.[39] For the CPAD RAFT agent, the reduction peak was located at −1.02 V, which is lower than that of the NAD$^+$ coenzyme by 0.27 V. Obviously, electroreduction of the NAD$^+$ coenzyme can efficiently mediate the reduction of the CPAD RAFT agent into radical species to initiate and sustain eRAFT polymerization.

Potential Window of the NAD$^+$-eRAFT Polymerization. The addition of an electron (1e) to the pyridinium ring of the NAD$^+$ coenzyme produces a radical species (Figure

https://doi.org/10.1021/acs.analchem.1c01766
Anal. Chem. 2021, 93, 9602−9608

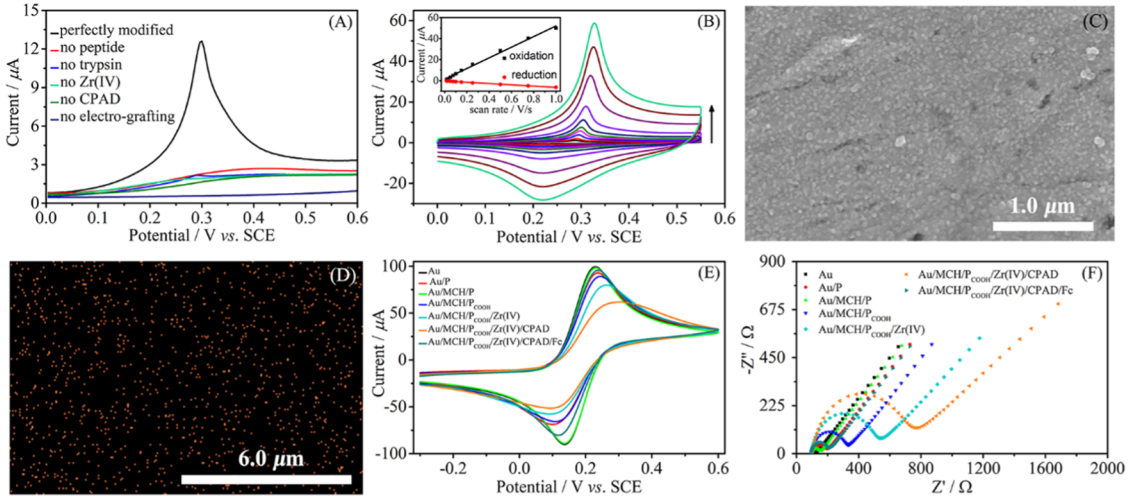

Figure 2. (A) SWVs of differently modified electrodes. (B) CVs of Au/MCH/P_{COOH}/Zr(IV)/CPAD/Fc at different scan rates (along the arrow direction, from 15 to 1000 mV/s). (C) SEM image and (D) Fe mapping of Au/MCH/P_{COOH}/Zr(IV)/CPAD/Fc. (E) CVs and (F) Nyquist plots of the sequentially modified electrodes in 5.0 mM $[Fe(CN)_6]^{3-/4-}$ containing 0.1 M KNO_3. The level of trypsin activity applied in the above experiments was 175 μU/mL.

S1),[39] which can reduce the CPAD RAFT agent into an anionic fragment and a free radical to initiate and sustain the eRAFT polymerization. At a more negative potential, the radical species can be further reduced (1e, $1H^+$) to dihydropyridine.[39] To precisely regulate the NAD^+-eRAFT polymerization, the reduction wave of the NAD^+ coenzyme at Au/MCH/P_{COOH}/Zr(IV)/CPAD in the FcMMA-free electrografting solution was collected. Reduction of the pyridinium ring of the NAD^+ coenzyme into a radical species resulted in a peak at −1.0 V (Figure S2), while the second reduction peak at a more negative potential (∼−1.18 V) corresponded to the formation of NADH, the reduced state of the NAD^+ coenzyme.[39] For better control over the polymerization process, the electrografting of ferrocenyl polymers through NAD^+-eRAFT polymerization should be performed at a potential not lower than −1.0 V.[34]

Effects of Experimental Conditions. Obviously, the cleavage efficiency of peptide substrates by trypsin is highly dependent on the surface coverage. With this in mind, the effect of the concentration of the peptide substrate on the electrochemical signal was studied (Figure S3A). As seen, the oxidation current increased with the increase of peptide concentration from 0.5 to 1.5 μM, while a further increase of peptide concentration would result in the decrease of oxidation current. Thus, the optimal concentration of the peptide substrate is 1.5 μM. This is understandable because the densely packed peptide layer at a higher concentration would seriously hinder the enzymatic cleavage by bulky trypsin molecules.

In addition, the effects of NAD^+ concentration (Figure S3B) and grafting potential (Figure S3C) on the oxidation current were studied. As observed, the optimal NAD^+ concentration and grafting potential were 1.0 μM and −0.85 V, respectively. This is as expected because a lower concentration of the radical form of the NAD^+ coenzyme would result in a slower grafting rate, while the presence of a much higher concentration would deteriorate the grafting due to the prevalence of side reactions.[34]

Characterization. SWVs of differently modified gold electrodes were collected to investigate the reliability of the oxidation current (Figure 2A). Au/MCH/P_{COOH}/Zr(IV)/CPAD/Fc was observed to show a high oxidation peak at about 0.3 V, in good agreement with the typical electrooxidation of Fc tags.[20,21] For the electrodes modified without peptide substrates, trypsin enzymes, Zr(IV) linkers, CPAD RAFT agents, or electrografting, no clear oxidation current could be observed. This is as expected because the absence of any one of these components would result in the unsuccessful modification of the electrode surface. Therefore, the oxidation current is reliable for the interrogation of trypsin activity.

CVs of Au/MCH/P_{COOH}/Zr(IV)/CPAD/Fc at different scan rates in 0.5 M $LiClO_4$ were applied to characterize the redox properties of ferrocenyl polymers. As expected, the oxidation and reduction peak currents correlated linearly with the scan rate (Figure 2B), in line with the surface-confined redox process.[20] Figure S4 shows the presence of Zr(IV) linkers on the electrode surface. Further, the densely packed particles (Figure 2C) and Fe elements (Figure 2D) confirmed the successful electrografting of a large number of ferrocenyl polymers from the electrode surface, indicative of the high efficiency of the NAD^+-eRAFT polymerization as a strategy for signal amplification.

CVs (Figure 2E) and EIS spectra (Figure 2F) were applied to characterize the sequential modification of the electrode surface. For the unmodified electrode, it exhibited fast interfacial charge-transfer (ICT) kinetics with low charge-transfer resistance (R_{ct}). As expected, the presence of steric hindrance caused by the self-assembled peptide substrates (Au/P) hampered the charge transfer, and the R_{ct} increased.[20,21] Subsequently, the backfilling of the peptide layer with MCH blocking agents (Au/MCH/P) facilitated the ICT kinetics and the R_{ct} decreased, likely due to the MCH-induced desorption of the nonspecifically adsorbed peptide substrates and the rearrangement of the covalently tethered ones from the flat-lying configuration into the upright configuration.[20] The tryptic cleavage of peptide substrates (without free carboxyl groups) generated the negatively charged carboxyl termini (Au/MCH/P_{COOH}), leading to a decrease in the ICT kinetics and an increase in the R_{ct}. The sequential modification of the Zr(IV) linkers (Au/MCH/

https://doi.org/10.1021/acs.analchem.1c01766
Anal. Chem. 2021, 93, 9602−9608

P_{COOH}/Zr(IV)) and the CPAD RAFT agents (Au/MCH/P_{COOH}/Zr(IV)/CPAD) resulted in an increase in both the ICT kinetics and the R_{ct}, which is consistent with previous reports.[20,21] After the electrografting of ferrocenyl polymers through the NAD^+-eRAFT polymerization, the recruitment of a large number of Fc redox tags onto the electrode surface would greatly facilitate the ICT kinetics, leading to a significant decrease in the R_{ct} (Au/MCH/P_{COOH}/Zr(IV)/CPAD/Fc).[20,21] From these observations, it can be concluded that the sequential modification of the electrode surface was successful.

Analytical Performance. Under the optimized conditions, the activity-dependent SWV curves of the as-constructed cleavage-based electrochemical trypsin biosensor were collected to investigate its analytical performance (Figure 3). The

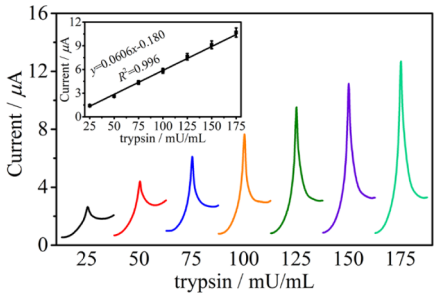

Figure 3. SWVs toward various trypsin activities and the plot of peak current versus trypsin activity. Error bars represent the standard deviations (n = 5).

peak current derived from the oxidation of Fc redox tags was observed to increase monotonously with the increase of trypsin activity. This is as expected because the presence of a higher level of trypsin activity would eventually result in the recruitment of more Fc redox tags. As a signal-on method, this trypsin biosensor could be less susceptible to false-positive results. The plot of peak current versus trypsin activity demonstrated that there is a good linear relationship between the peak current and trypsin activity from 25 to 175 μU/mL, with a correction coefficient (R^2) of 0.996. The regression equation of the calibration plot was $y = 0.0606x - 0.180$, in which y represents the peak current in μA and x represents the level of trypsin activity in μU/mL. The limit of detection (LOD) was calculated, according to the well-established $3\sigma_{blank}$/slope criterion, to be 18.2 μU/mL, equaling to ~72.8 pg/mL in mass concentration or ~3.05 pM in molar concentration. Table S1 shows that the obtained LOD is superior or at least comparable to those of most of the previously reported methods, demonstrating that the electrografting of ferrocenyl polymers through the NAD^+-eRAFT polymerization is highly applicable to the interrogation of trypsin activity at ultralow levels.

In addition, the values of the intra-assay and inter-assay coefficients of variation (COVs, n = 5) for the interrogation of trypsin activity at a level of 175 μU/mL were about 5.3 and 5.8%, respectively. Therefore, the reproducibility of the as-constructed electrochemical trypsin biosensor is satisfactory.

After storing at 4 °C for 2 weeks, the peak current toward 175 μU/mL trypsin decreased by about 5.4% (n = 5). Thus, the as-modified electrodes possessed satisfactory long-term storage stability.

Selectivity. To investigate the selectivity of the as-constructed electrochemical trypsin biosensor, the peak currents toward six other proteins were collected (Figure 4A). Although the concentrations of these control components were as high as 10 times that of trypsin, none of them could result in an obvious peak current as trypsin did. In particular, the coexistence of these nontargeted proteins with trypsin would not interfere with the electrochemical interrogation of trypsin activity. Such a high selectivity can be, to a significant extent, ascribed to the high specificity of an enzyme to its substrate, while the enzymatic activities are also highly dependent on the buffer solutions (e.g., pH and cofactors).

Inhibitor Screening. As potential therapeutic drugs, trypsin inhibitors are of great value in targeted therapy. To investigate the applicability of the as-constructed cleavage-based electrochemical trypsin biosensor in inhibitor screening, the proof-of-concept experiment was conducted with BBI. Prior to the addition onto the electrode surface, trypsin solutions with enzyme activity at a level of 175 μU/mL were incubated with BBI at 37 °C for 15 min. As shown in Figure 4B, the presence of a higher dose of BBI would result in a lower peak current. This observation is as expected because lower tryptic activity would result in the generation of fewer carboxyl termini and consequently the recruitment of fewer Fc redox tags. From the corresponding curve of the inhibition efficiency versus BBI dose, the value of the half-maximal inhibitory dose (IC_{50}) was estimated to be 3.54 ng/mL. Consequently, the as-constructed cleavage-based electrochemical trypsin biosensor is applicable to inhibitor screening.

Interrogation of Trypsin Activity in Human Urine Samples. To demonstrate the applicability of the as-constructed cleavage-based electrochemical trypsin biosensor in the in vitro diagnosis (IVD), it was applied to interrogate trypsin activity in the spiked human urine samples from healthy individuals. It is noteworthy that trypsin is absent from

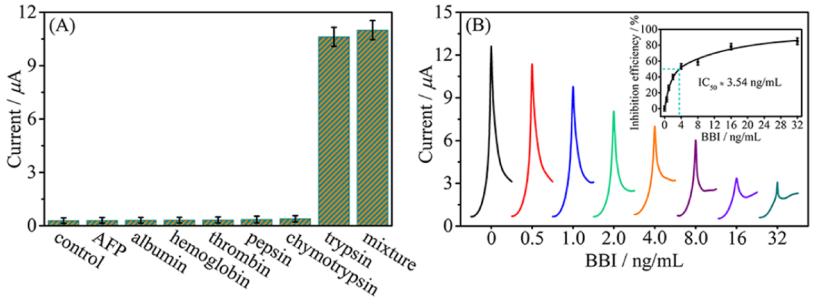

Figure 4. (A) Peak currents toward trypsin and the control proteins. Trypsin, 0.7 ng/mL (~175 μU/mL); others, 7.0 ng/mL. (B) SWVs toward various BBI doses and the plot of inhibition efficiency versus BBI dose. Error bars represent standard deviations (n = 5).

https://doi.org/10.1021/acs.analchem.1c01766
Anal. Chem. 2021, 93, 9602−9608

the urine of healthy individuals.[40] Summarized in Table 1 are the results obtained from the well-established standard addition experiments. The recoveries were within the range of 95.4−105.6%, and the relative standard deviations (RSDs) ranged from 5.3 to 5.7%. Obviously, the presence of the complex urine matrices would not interfere with the electrochemical interrogation of trypsin activity. The satisfactory anti-interference capability confirmed the applicability of the trypsin biosensor for potential IVD applications.

Table 1. Interrogation of Trypsin Activity in Human Urine Samples

sample	added (μU/mL)	found (μU/mL)	recovery (%)	RSD (%) (n = 5)
1	25	26.4	105.6	5.7
2	100	104.5	104.5	5.5
3	175	167	95.4	5.3

CONCLUSIONS

In summary, the coenzyme-mediated electrografting of ferrocenyl polymers has been successfully demonstrated as a novel strategy for signal amplification for the electrochemical interrogation of trypsin activity at ultralow levels. For signal amplification, the electrografting of ferrocenyl polymers through NAD^+-eRAFT polymerization involves only a two-step operation (i.e., the labeling of RFAT agents and the potentiostatic electrografting under mild conditions); obviously, it is low-cost and easy to operate. The electrografting of ferrocenyl polymers recruits a considerable amount of Fc redox tags for signal output, allowing for the signal-on interrogation of trypsin activity at ultralow levels. Meanwhile, the cleavage-based method operating by the use of synthetic peptides as immobilized recognition elements enables the highly selective interrogation of trypsin activity instead of the abundance and, as a result, the results are more clinically relevant. The results also demonstrated that it can be applied to inhibitor screening and the interrogation of trypsin activity in the presence of complex urine matrices. Taking these into consideration, the as-constructed cleavage-based electrochemical trypsin biosensor holds great promise in diagnostic and therapeutic applications.

ASSOCIATED CONTENT

Supporting Information

The Supporting Information is available free of charge at https://pubs.acs.org/doi/10.1021/acs.analchem.1c01766.

One-electron reduction of the NAD^+ coenzyme into a radical species (Figure S1); potential window of the NAD^+-eRAFT polymerization (Figure S2); effects of experimental conditions (Figure S3); elemental mapping of the Zr(IV) linker (Figure S4); and analytical performance of different cleavage-based methods for trypsin activity interrogation (Table S1) (PDF)

AUTHOR INFORMATION

Corresponding Author

Li Niu − *Center for Advanced Analytical Science, School of Chemistry and Chemical Engineering, Guangzhou University, Guangzhou 510006, P. R. China;* orcid.org/0000-0003-3652-2903; Phone: +86-020-39366902; Email: lniu@gzhu.edu.cn

Authors

Qiong Hu − *Center for Advanced Analytical Science, School of Chemistry and Chemical Engineering, Guangzhou University, Guangzhou 510006, P. R. China;* orcid.org/0000-0001-6360-1813

Luofeng Su − *Center for Advanced Analytical Science, School of Chemistry and Chemical Engineering, Guangzhou University, Guangzhou 510006, P. R. China*

Zhuohua Chen − *Center for Advanced Analytical Science, School of Chemistry and Chemical Engineering, Guangzhou University, Guangzhou 510006, P. R. China*

Yanyu Huang − *Center for Advanced Analytical Science, School of Chemistry and Chemical Engineering, Guangzhou University, Guangzhou 510006, P. R. China*

Dongdong Qin − *Center for Advanced Analytical Science, School of Chemistry and Chemical Engineering, Guangzhou University, Guangzhou 510006, P. R. China*

Complete contact information is available at: https://pubs.acs.org/10.1021/acs.analchem.1c01766

Author Contributions

All authors have given approval to the final version of the manuscript.

Notes

The authors declare no competing financial interest.

ACKNOWLEDGMENTS

This work was supported by the National Natural Science Foundation of China (21904026) and the start-up funding from Guangzhou University (RQ2021011).

REFERENCES

(1) Rick, W. Trypsin. In *Methods of Enzymatic Analysis*, 2nd ed.; Bergmeyer, H. U., Ed.; Academic Press: New York, 1974; Vol. 2, pp 1013−1024.

(2) See, W. A.; Smith, J. L. *Transplantation* **1991**, *52*, 630−633.

(3) Elias, E.; Wood, T.; Redshaw, M. *Lancet* **1977**, *310*, 66−68.

(4) Zaccheo, B. A.; Crooks, R. M. *Anal. Chem.* **2011**, *83*, 1185−1188.

(5) Zhou, S.; Wang, L.; Chen, X.; Guan, X. *ACS Sens.* **2016**, *1*, 607−613.

(6) Goldberg, J. M.; Chen, X.; Meinhardt, N.; Greenbaum, D. C.; Petersson, E. J. *J. Am. Chem. Soc.* **2014**, *136*, 2086−2093.

(7) Lefkowitz, R. B.; Schmid-Schönbein, G. W.; Heller, M. J. *Electrophoresis* **2010**, *31*, 2442−2451.

(8) Zhao, L.; Wang, T.; Wu, Q.; Liu, Y.; Chen, Z.; Li, X. *ACS Appl. Mater. Interfaces* **2017**, *9*, 3400−3410.

(9) He, M. Q.; Chen, S.; Yao, K.; Meng, J.; Wang, K.; Yu, Y. L.; Wang, J. H. *Anal. Chem.* **2020**, *92*, 1395−1401.

(10) Dai, H.; Chen, S.; Li, Y.; Zeng, B.; Zhang, S.; Hong, Z.; Lin, Y. *Biosens. Bioelectron.* **2017**, *92*, 687−694.

(11) Stoytcheva, M.; Zlatev, R.; Cosnier, S.; Arredondo, M.; Valdez, B. *Biosens. Bioelectron.* **2013**, *41*, 862−866.

(12) Liu, H.; Yin, H.; Dong, Y.; Ding, H.; Chu, X. *Analyst* **2020**, *145*, 2204−2211.

(13) Hu, J.; Liu, F.; Ju, H. *Anal. Chem.* **2015**, *87*, 4409−4414.

(14) Wu, Z.; Liu, Y.; Liu, Y.; Xiao, H.; Shen, A.; Zhou, X.; Hu, J. *Biosens. Bioelectron.* **2015**, *65*, 375−381.

(15) Li, M.; Rauf, A.; Guo, Y.; Kang, X. *ACS Sens.* **2019**, *4*, 2854−2857.

(16) Cao, Y.; Yu, J.; Bo, B.; Shu, Y.; Li, G. *Biosens. Bioelectron.* **2013**, *45*, 1−5.

(17) Adjémian, J.; Anne, A.; Cauet, G.; Demaille, C. *Langmuir* **2010**, *26*, 10347−10356.
(18) González-Fernández, E.; Avlonitis, N.; Murray, A. F.; Mount, A. R.; Bradley, M. *Biosens. Bioelectron.* **2016**, *84*, 82−88.
(19) Liang, R. P.; Tian, X. C.; Qiu, P.; Qiu, J. D. *Anal. Chem.* **2014**, *86*, 9256−9263.
(20) Hu, Q.; Bao, Y.; Gan, S.; Zhang, Y.; Han, D.; Niu, L. *Biosens. Bioelectron.* **2020**, *165*, No. 112358.
(21) Hu, Q.; Gan, S.; Bao, Y.; Zhang, Y.; Han, D.; Niu, L. *Anal. Chem.* **2020**, *92*, 15982−15988.
(22) Wu, Y.; Wei, W.; Liu, S. *Acc. Chem. Res.* **2012**, *45*, 1441−1450.
(23) Hu, Q.; Su, L.; Mao, Y.; Gan, S.; Bao, Y.; Qin, D.; Wang, W.; Zhang, Y.; Niu, L. *Biosens. Bioelectron.* **2021**, *178*, No. 113010.
(24) Wu, Y.; Liu, S.; He, L. *Anal. Chem.* **2009**, *81*, 7015−7021.
(25) Yuan, L.; Wei, W.; Liu, S. *Biosens. Bioelectron.* **2012**, *38*, 79−85.
(26) Hu, Q.; Gan, S.; Bao, Y.; Zhang, Y.; Han, D.; Niu, L. *J. Mater. Chem. B* **2020**, *8*, 3327−3340.
(27) Hu, Q.; Wang, Q.; Sun, G.; Kong, J.; Zhang, X. *Anal. Chem.* **2017**, *89*, 9253−9259.
(28) Strover, L. T.; Postma, A.; Horne, M. D.; Moad, G. *Macromolecules* **2020**, *53*, 10315−10322.
(29) Perrier, S. *Macromolecules* **2017**, *50*, 7433−7447.
(30) Hu, Q.; Bao, Y.; Gan, S.; Zhang, Y.; Han, D.; Niu, L. *Anal. Chem.* **2020**, *92*, 3470−3476.
(31) He, P.; Lou, X.; Woody, S. M.; He, L. *ACS Sens.* **2019**, *4*, 992−1000.
(32) Hu, Q.; Han, D.; Gan, S.; Bao, Y.; Niu, L. *Anal. Chem.* **2018**, *90*, 12207−12213.
(33) Nothling, M. D.; Fu, Q.; Reyhani, A.; Allison-Logan, S.; Jung, K.; Zhu, J.; Kamigaito, M.; Boyer, C.; Qiao, G. G. *Adv. Sci.* **2020**, *7*, No. 2001656.
(34) Hu, Q.; Kong, J.; Han, D.; Zhang, Y.; Bao, Y.; Zhang, X.; Niu, L. *Anal. Chem.* **2019**, *91*, 1936−1943.
(35) Wang, Y.; Fantin, M.; Park, S.; Gottlieb, E.; Fu, L.; Matyjaszewski, K. *Macromolecules* **2017**, *50*, 7872−7879.
(36) Strover, L. T.; Cantalice, A.; Lam, J. Y.; Postma, A.; Hutt, O. E.; Horne, M. D.; Moad, G. *ACS Macro Lett.* **2019**, *8*, 1316−1322.
(37) Lorandi, F.; Fantin, M.; Shanmugam, S.; Wang, Y.; Isse, A. A.; Gennaro, A.; Matyjaszewski, K. *Macromolecules* **2019**, *52*, 1479−1488.
(38) Sang, W.; Xu, M.; Yan, Q. *ACS Macro Lett.* **2017**, *6*, 1337−1341.
(39) Schmakel, C. O.; Santhanam, K. S. V.; Elving, P. J. *J. Am. Chem. Soc.* **1975**, *97*, 5083−5092.
(40) Zhao, D.; Chen, C.; Zhao, J.; Sun, J.; Yang, X. *Sens. Actuators, B* **2017**, *247*, 392−399.

https://doi.org/10.1021/acs.analchem.1c01766
Anal. Chem. 2021, 93, 9602−9608